Radiation Physics and Chemistry 81 (2012) 362–369

Contents lists available at SciVerse ScienceDirect

Radiation Physics and Chemistry

journal homepage: www.elsevier.com/locate/radphyschem

The effect of gamma irradiation on electrical and dielectric properties of organic-based Schottky barrier diodes (SBDs) at room temperature

Habibe Uslu [a,*], Mert Yıldırım [b], Şemsettin Altındal [c], Perihan Durmuş [c]

[a] Department of Electric and Electronic Engineering, Faculty of Engineering, Karabük University, 78050, Karabük, Turkey
[b] Department of Physics, Faculty of Science, Düzce University, 81620 Düzce, Turkey
[c] Department of Physics, Faculty of Science, Gazi University, 06500 Ankara, Turkey

ARTICLE INFO

Article history:
Received 21 September 2010
Accepted 21 December 2011
Available online 5 January 2012

Keywords:
Organic-based SBDs
Radiation effects
Dielectric properties
AC electrical conductivity
Interface states
Series resistance

ABSTRACT

The effect of ^{60}Co (γ-ray) irradiation on the electrical and dielectric properties of Au/Polyvinyl Alcohol (Ni,Zn-doped)/n-Si Schottky barrier diodes (SBDs) has been investigated by using capacitance-voltage (C-V) and conductance-voltage (G/ω-V) measurements at room temperature and 1 MHz. The real capacitance and conductance values were obtained by eliminating series resistance (R_s) effect in the measured capacitance (C_m) and conductance (G_m) values through correction. The experimental values of the dielectric constant (ε'), dielectric loss (ε''), loss tangent ($tan\delta$), ac electrical conductivity (σ_{ac}) and the real (M') and imaginary (M'') parts of the electrical modulus were found to be strong functions of radiation and applied bias voltage, especially in the depletion and accumulation regions. In addition, the density distribution of interface states (N_{ss}) profile was obtained using the high-low frequency capacitance (C_{HF}–C_{LF}) method for before and after irradiation. The N_{ss}-V plots give two distinct peaks for both cases, namely before radiation and after radiation, and those peaks correspond to two different localized interface states regions at M/S interface. The changes in the dielectric properties in the depletion and accumulation regions stem especially from the restructuring and reordering of the charges at interface states and surface polarization whereas those in the accumulation region are caused by series resistance effect.

1. Introduction

In general, there are several possible sources of error in the electrical and dielectric properties of SBDs, which cause deviation from the ideal case. These errors could be related to some parameters like interface state density localized at metal/semiconductor (M/S) interface, series resistance of the device, interfacial insulator/polymer layer and its homogeneity, and fabrication process of the device. Hence, these parameters should be taken into account in the calculations. In recent years, considerable attention has been given to the fabrication of organic semiconductor devices, as well as to their dielectric and electrical characterization, because of their wide variety of electronic and electro-optical properties (Akkılıç et al., 2007; Aydın et al., 2006; Aydoğan et al., 2005; Dökme et al., 2010; Gupta and Singh, 2004; Güllü et al., 2008a,2008b; Shehap et al., 1998; Taşcıoğlu et al., 2010; Vural et al., 2007). In addition, when the polyvinyl alcohol (PVA) is doped with metals, such as Ni, Zn and Co, it will lead to an improvement in the polymer behavior of polymer chains and it often brings about new progresses in SBDs performance.

When organic films are inserted between metal and an inorganic semiconductor, they modify both electrical and dielectric properties of SBDs. When a bias voltage is applied across the diode, the combination of the interfacial insulator or polymer layer, depletion layer and series resistance of the diode share this applied bias voltage. Interface states at M/S interface can be divided into two main groups and are dependent on the thickness of the interfacial layer (δ). These surface states act as recombination centers, which provide a tunneling path for the carriers. One of the groups communicates with the metal rapidly if the value of δ is lower than about 30 Å, the other group communicates with the semiconductor if the value of δ is higher than about 30 Å (Card and Rhoderick, 1971).

Especially semiconductor based devices such as Schottky barrier diodes (SBDs), metal-insulator/oxide-semiconductor (MIS or MOS) structures and solar cells have been used in many satellites and they played an importance role in a wide range of communications, broadcast, meteorological, scientific research, space development applications and other industrial areas. Development of electronic sensors, solar cells, MS or MIS type SBDs and MOS structures with stable performance in strongly ionizing

* Corresponding author. Tel.: +90 370 4332021; fax: +90 370 4333290.
E-mail address: habibeuslu@karabuk.edu.tr (H. Uslu).

0969-806X/$ - see front matter © 2011 Elsevier Ltd. All rights reserved.
doi:10.1016/j.radphyschem.2011.12.029

radiation fields is also essentials to improving the reliability of atomic power plants and nuclear fusion systems. Since radiation in space is severe, considerable amount of lattice defects are induced in semiconductors due to irradiations and these defects causes degradation in these devices [Yamaguchi, 2001]. Hence, electronic/semiconductor devices (electronic sensors, solar cells, MS or MIS type SBDs and MOS structures) that can be used in strongly ionizing radiation fields and at high temperatures must be developed to improve the reliability of the satellites or plants. In addition, high-energy particles, such as ^{60}Co γ-ray, high level electrons, neutrons or ions, irradiated enter these devices or exposure dose greater than a kilorad, the considerable amount of lattice defects such as vacancies, interstitials; complex defects are induced in the semiconductor material. These defects act as a recombination centers trapping the generated carriers (electrons and/or holes). In this sense, it is very important to fabricate radiation-resistant devices. Therefore, it is of interest to investigate the damage defect centers on the performance of these types of semiconductor devices. These samples can be used both in space and industrial applications. On the other hand, the effect of radiation on these devices changes from one device to another, for example; the effect of radiation is more effective on solar cells and SBDs without interfacial insulator layer rather than MOS structures.

Moreover, radiation generates electron-hole pairs in the interfacial insulator or organic PVA layer that subsequently interact with trapping sites within the interfacial layer. These radiation-generated electrons either recombine with the holes or move out of the interfacial layer. On the other hand, the radiation generated holes may diffuse in the interfacial layer, but are less mobile than the electrons; many stationary traps are also present. When there is an electric field presence, the electrons will readily move out of the interfacial layer, and the trapping of holes becomes considerably enhanced (Zainninger and Holmes-Siedle, 1967).

Recently, it has been found by researchers that radiation response of MIS and MOS structures changes significantly when these structures are exposed to irradiation stress treatments (Chauhan and Chakrabarti, 2002; El-Sayed et al., 2004; Feteha et al., 2002; Gomaa, 2001; Gökçen et al., 2008; Jayavel et al., 2000; Karataş et al., 2009; Karataş and Türüt, 2010; Radwan, 2007; Uğurel et al., 2008; Umana-Membreno et al., 2003; Ma, 1989; Oldham and McLean, 2003; Taşcıoğlu et al., 2009; Uslu et al., 2011; Winokur et al., 1984,1976; Yufen et al., 1994; Zainninger and Holmes-Siedle, 1967). They observed that the influence of high-level radiation such as γ-rays on these semiconductor devices produces lattice defects and hence quasi-stable changes happen in the electrical and dielectric properties of such devices. Among those researchers Ma (Ma, 1989), Winokur et al. (Winokur et al., 1984,1976) and Zainninger et al. (Zainninger and Holmes-Siedle, 1967) were the first ones to make a systematic observation of the after-irradiation behavior of inter-band radiation-induced interface states (N_{ss}) in MIS structures. In the case of polymers, the incident energic particles transfer their energy to the dielectrics through the interaction with polymeric molecules. This causes the ionization or excitation of macromolecules, and leading to the free radical chain reactions, thus changing the molecular and atomic structure (Radwan, 2007). The inorganic-organic semiconductor devices such as metal-polymer-semiconductor (MPS) type SBDs, light-emitting diodes (LEDs), and solar cells have potential advantages compared to the traditional inorganic devices. Therefore, the radiation effects on polymers after and during the ionizing radiation are investigated by more and more researchers using different measurement methods such as current-voltage (*I-V*), admittance spectroscopy method (*C-V* and G/ω-*V*) and deep-level transient spectroscopy (DLTS) (Güllü et al., 2008a,2008b; Uslu et al., 2011; Yufen et al., 1994). The behaviors of electrical and dielectric properties of MPS structures are similar to the MIS type SBDs, therefore same methods can be used to investigate these structures.

Polyvinyl alcohol (PVA) used in this study is the most interesting material among the other polymers in terms of its large scale applications such as surgical devices, sutures, implantation and synthetic articulate cartilages in reconstructive point surgery (Ahmed and Abo-Ellil, 1998). What makes PVA an interesting material is that it is water-soluble and biocompatible, which are mainly due to hydrogen bonds between hydroxyl groups on the chain and water molecules or biomolecules (Ahmed and Abo-Ellil, 1998; Kubo et al., 2009). Moreover, PVA crystallizes in some solvents such as water and mixture of dimethyl sulfoxide, this leads to the formation of physical PVA gels, which are used in various industrial products such as contact lens, disposable diaper, and sewage treatment. PVA is normally a poor electrical conductor; however it becomes conductive upon doping with some dopants (Co, Ni, Zn). Therefore, the study of the electrical and dielectric properties of these materials is of particular interest in this report. Although high-frequency ($f > 500$ kHz) *C-V* and G/ω-*V* measurements are not relatively carried out easily and rapidly, admittance spectroscopy method can yield interesting and meaningful results (Ma, 1989; Winokur et al., 1984; Nicollian and Brews, 1976; Zainninger and Holmes-Siedle, 1967).

In this study, we measured both forward and reverse bias *C-V* and G/ω-*V* characteristics at room temperature and 1 MHz before and after irradiation in order to achieve a better understanding of the effects of ^{60}Co γ-ray irradiation (22 kGy) on the electrical and dielectric properties of Au/PVA (Ni, Zn-doped)/n-Si structures. The voltage dependence of R_s and N_{ss} profiles, the real (ε') and imaginary (ε'') parts of the dielectric constant, lost tangent ($tan\delta$), ac electrical conductivity (σ_{ac}) and real (M') and imaginary (M'') parts of the electric modulus of the structure were also investigated before and after irradiation.

2. Experimental detail

0.5 g of nickel acetate and 0.25 g of zinc acetate was mixed with 1 g of polyvinyl alcohol (PVA), molecular weight=72 000 and 9 ml of de-ionized water. After vigorous stirring for 2 h at 50 °C, a viscous solution of PVA (Ni,Zn-doped) was obtained. The substrate used in this study is P-doped single crystal Si wafer having a thickness 350 μm. The native oxide on the front surface of the substrate was cleaned in a mix of a peroxide-ammoniac solution in 10 min and then in H_2O+HCl solution and then was rinsed in de-ionized water of resistivity of 18 MΩ cm. using an ultrasonic bath for 15 min before making contacts. The conductivity of PVA (Ni, Zn-Doped) polymer was measured 1.21×10^{-6} S cm^{-1} using four point probe technique (ENTEK Company). A contact on back contact to n-type Si wafer was formed by thermal evaporation of Au metal and was thermally treated onto whole back side of Si wafer at a pressure about 10^{-6} Torr in high vacuum system. The solution of the PVA (Ni, Zn-Doped) was homogenized for 1.5 h by mixing with rotation before the deposition. PVA (Ni,Zn-Doped) nanofiber film on n-Si substrate was coated by electrospinning technique. Electrospinning process utilizes electrical force to produce polymer fibers. Electrospinning is especially interesting in that it is simple and cost effective [Altındal and Uslu, 2011; Dökme et al., 2010; Uslu et al., 2010; Taşcıoğlu et al., 2010; Tunç et al., 2011]. Electrospinning setup consists of four major components; the high-voltage power supply, the spinneret, the syringe pump and the electrically conductive collector. Also, a simple illustration of the electrospinning system is given in Fig. 1. The composite solution for spinning was loaded into a 10 mL hypodermic stainless steel syringe with a needle (0.8 mm in diameter and 38 mm length) connected to a digitally controlled pump (New Era), which

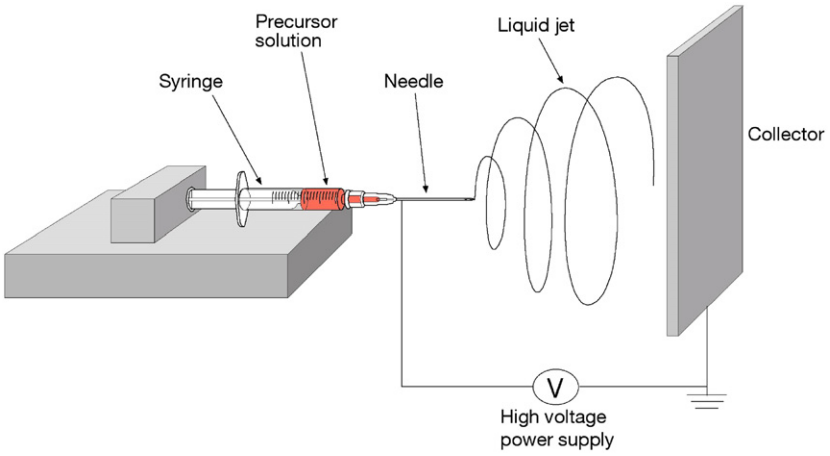

Fig. 1. Schematic representation of the electrospinning process.

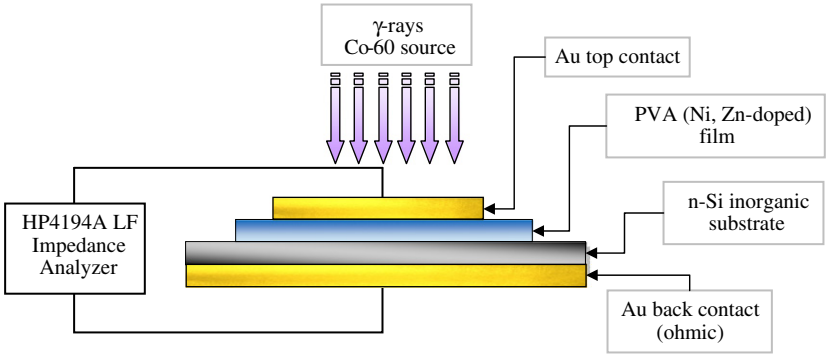

Fig. 2. Schematic model of the Au/Polyvinyl Alcohol (Ni, Zn-doped)/n-Si SBD under ^{60}Co (γ-ray) irradiation.

provides a constant feeding rate. The positive electrode of a high-voltage power supply (SP- 30P) was placed on to the top of the needle. The negative electrode was connected to a metallic stationary collector wrapped with aluminum foil and served as a counter electrode and spun under 20 kV. The working distance (WD) between the tip of the syringe needle and the collector was 19,5 cm. Composite fibers were collected on Si wafer on the aluminum foil, dried at 60 °C under vacuum for 10 h. The solvent evaporated and a charged fiber was deposited onto the Si wafer as a nonwoven mat. After spinning, the Schottky/rectifier contacts were coated by evaporation with Au dots with a diameter of about 1.0 mm (diode area $=7{,}85\times10^{-3}$ cm^2).

The *C-V* and *G/ω-V* measurements of structures are carried out at 1 MHz before and after ^{60}Co γ-ray source by using HP 4194A LF impedance analyzer (5 Hz–13 MHz) and a small sinusoidal signal of 40 mV$_{p-p}$ from the external pulse generator is applied to the sample in order to meet the requirement (Nicollian and Brews, 1976). Also, the schematic representation of the experimental setup is given in Fig. 2. The fabricated Au/PVA (Ni, Zn-doped)/n-Si structures were exposed to ^{60}Co γ-radiation at a dose rate of 2.12 kGy/h in water at room temperature while there was no external electric field applied. All measurements were carried out with the help of a microcomputer through an IEEE-488 ac/dc converter card at room temperature.

3. Results and discussion

3.1. Electrical characteristics

The plots of the measured *C-V* and *G/ω-V* of the Au/Polyvinyl Alcohol (Ni, Zn-doped)/n-Si SBDs reflect the data measured before and after irradiation at room temperature and 1 MHz and they are given in Fig. 3 (a) and (b), respectively. As shown in Fig. 3 (a) and (b), both *C-V* and *G/ω-V* characteristics exhibit inversion, depletion and accumulation regions. The range of the applied bias voltage is −4 V to 5 V. It can be seen in Fig. 3 (a) that the values of C increase under the effect of γ radiation in the inversion and accumulation regions whereas they decrease in the depletion region. Also, there is a peak in both plots (before and after irradiation) of *C-V* at about 1.5 V because of the effect of R_s. Such behavior shows that the N_{ss} is the significant parameter in the depletion and weak accumulation regions whereas the significant parameter in the strong accumulation region is R_s. As can be seen in Fig. 3 (a) and (b), there is a discrepancy in the values of C and G/ω due to radiation induced interface states.

In order to eliminate the effect of R_s on C and G/ω, R_s-V plots were obtained from the *C-V* and *G/ω -V* measurements at 1 MHz using the following equation (Nicollian and Brews, 1976) and are given in Fig. 4.

$$R_s = \frac{G_m}{G_m^2+(\omega C_m)^2} \tag{1}$$

where C_m and G_m are the values of measured capacitance and conductance at a given bias voltage, respectively. These significant values require that special attention should be given to the effects of R_s in the applications of the admittance-based *C-V* and *G/ω-V* measurement methods. As can be seen in Fig. 4, before and after radiation plots of R_s give a peak at about 0.5 V. The magnitude of the peak decreases under the radiation effect and the position of the peak shifts slightly to the high forward bias region. It is clearly seen in Fig. 4 that R_s is almost independent of the applied bias voltage in the accumulation region while there is

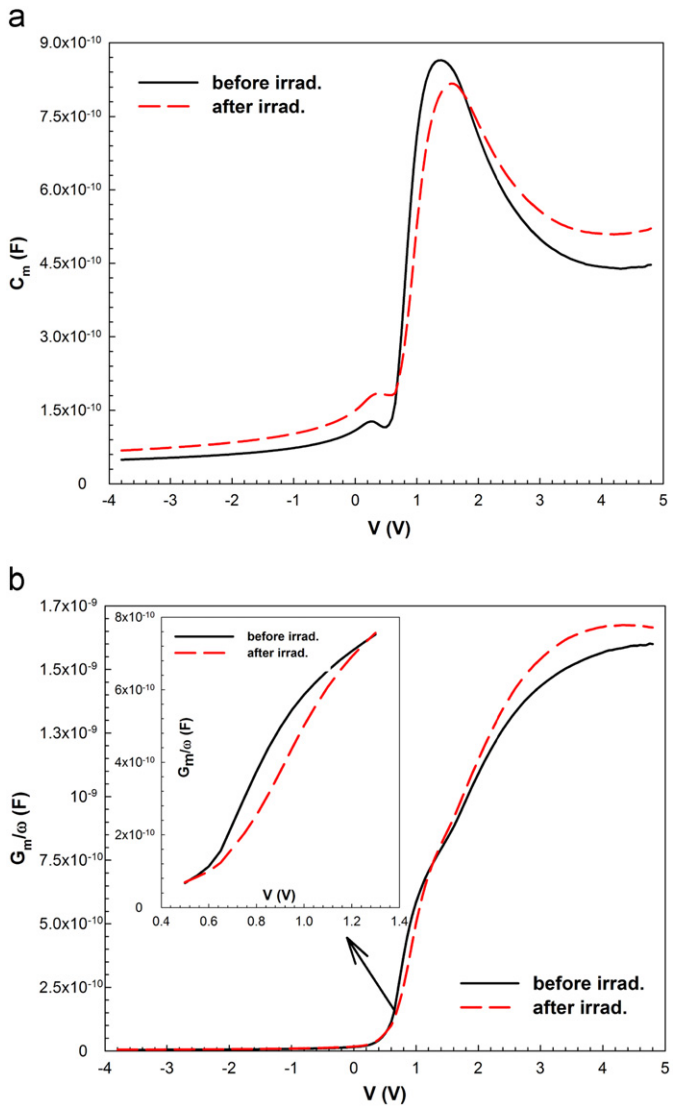

Fig. 3. Measured **(a)** *C-V* **(b)** G/ω-*V* characteristics of Au/Polyvinyl Alcohol (Ni, Zn-doped)/n-Si SBD before and after radiation.

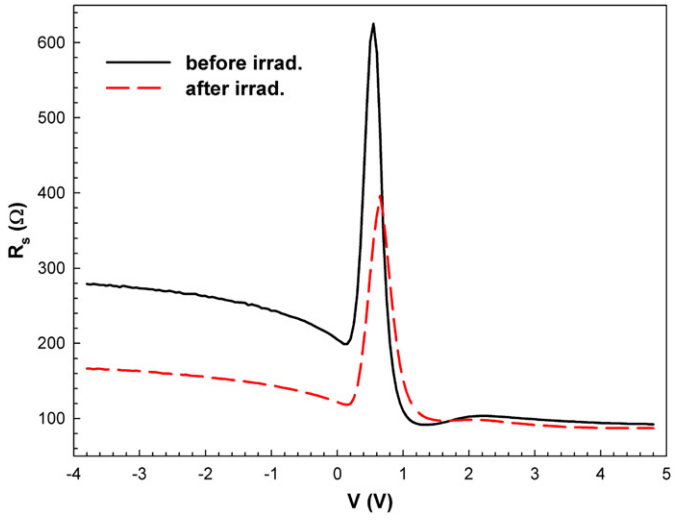

Fig. 4. R_s characteristics of Au/Polyvinyl Alcohol (Ni, Zn-doped)/n-Si SBD before and after radiation.

a considerable decrease in the inversion region with the effect of radiation. We considered that the trap charges have enough energy to escape from the traps located at M/S interface in the inversion region of Si band gap.

The obtained series resistance values are used to correct the measured *C-V* and G/ω-*V* values. Therefore, measured capacitance and conductance values were corrected by eliminating the effect of R_s in order to obtain the real capacitance C_c and conductance G_c/ω values of the diode under reverse and forward bias. The corrected capacitance C_c and conductance G_c values are calculated using the following relations (Nicollian and Brews, 1976):

$$C_c = \frac{(G_m^2 + (\omega C_m)^2) C_m}{a^2 + (\omega C_m)^2} \tag{2}$$

$$G_c = \frac{(G_m^2 + (\omega C_m)^2) a}{a^2 + (\omega C_m)^2} \tag{3}$$

where $a = G_m - (G_m^2 + (\omega C_m)^2) R_s$. After the correction is made, *C-V* and G/ω-*V* plots with their corrected versions before and after irradiation are given in Fig. 5 (a) and (b), respectively. As can be seen in these figures, when the correction was made on the *C-V* plot, the values of C_c increase considerably especially in the depletion and accumulation regions.

On the other hand, after the correction G_c/ω-*V* plots give two peaks; one of which is in the depletion region proving that the charge transfer can take place through the interface. The first peak

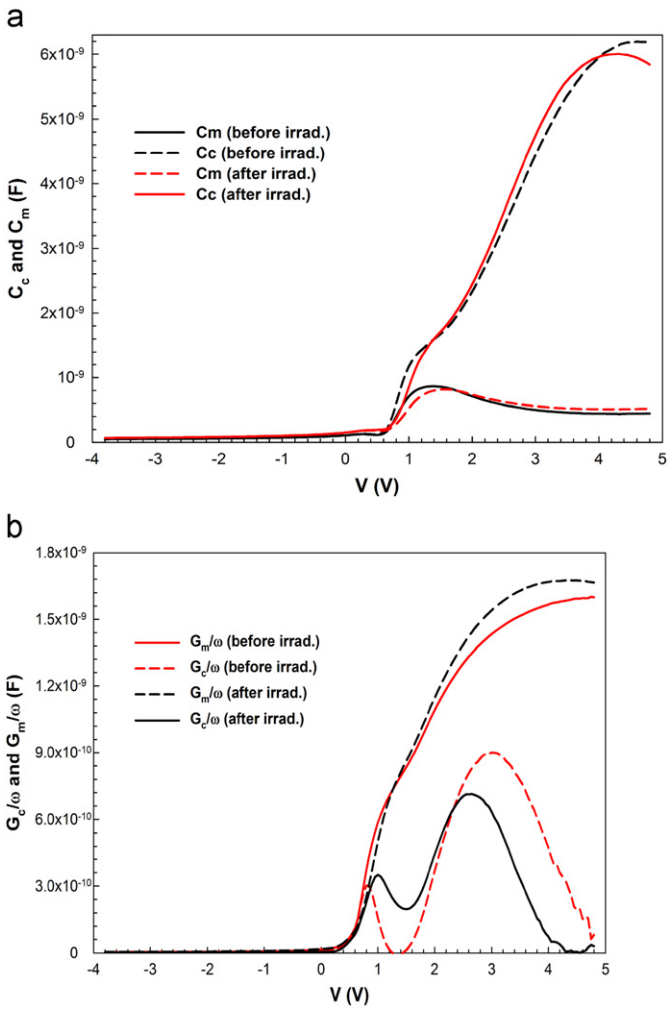

Fig. 5. Plots of the voltage dependent **(a)** C_c-*V* and **(b)** G_c/ω-*V* of Au/Polyvinyl Alcohol (Ni, Zn-doped)/n-Si SBD before and after radiation.

is located at the low forward bias region and the second peak is located at the high forward bias region. Moreover, the first peak shifts to the high forward bias region while the second peak shifts to the low forward bias region under the radiation effect.

The changes in C-V and G/ω-V plots can be attributed to restructuring and reordering of interface charges located at M/S interface under radiation effect. Both values of C and G/ω increase in the accumulation region under radiation effect. This increase in C and G/ω values is also attributed to the increase in ε' and ε'' values.

There are several methods, which have been suggested to determine the N_{ss} profile of MIS type SBDs (Castange and Vapaille, 1971; Çakar et al., 2002; Hill and Coleman, 1980; Nicollian and Brews, 1976). Among them the advantageous one is the high-low frequency capacitance (C_{HF}-C_{LF}) method (Castange and Vapaille, 1971), since it permits determination of many properties of the interfacial layer, the semiconductor substrate and interface easily. With this method, N_{ss} can be extracted from its capacitance contribution to the measured experimental C-V curve. The equivalent capacitance is the series connection of C_{ox} and surface charge capacitance C_{sc}. In this study, we used C_{HF}-C_{LF} method for before and after irradiation. N_{ss} values are obtained using the following equation,

$$N_{ss}=\frac{1}{qA}\left[\left(\frac{1}{C_{LF.}}-\frac{1}{C_{ox}}\right)^{-1}-\left(\frac{1}{C_{HF}}-\frac{1}{C_{ox}}\right)^{-1}\right] \tag{4}$$

where C_{LF} and C_{HF} are the values of capacitance at low and high frequency, respectively. The density distribution of N_{ss} profile as function of bias voltage was calculated from Eq. (4) and is given in Fig. 6. As shown in Fig. 6, before and after irradiation plots of N_{ss} give two peaks at about 0.5 V and 2 V, respectively and the magnitude of the second peak increases under the radiation effect due to the radiation induced interface states and the peak value is about 3.4×10^{12} eV^{-1} cm^{-2}. Devices with this order of interface states are more suitable for the fabrication of electronic devices. Moreover, these results show that the fabricated Au/n-Si diodes with Polyvinyl Alcohol (Ni, Zn-doped) interfacial layer are more resistant to the radiation.

3.2. Dielectric properties

The dielectric constant (ε'), dielectric loss (ε''), loss tangent ($tan\delta$), ac electrical conductivity (σ_{ac}) and real (M') and imaginary (M'') parts of electric modulus were calculated from the obtained

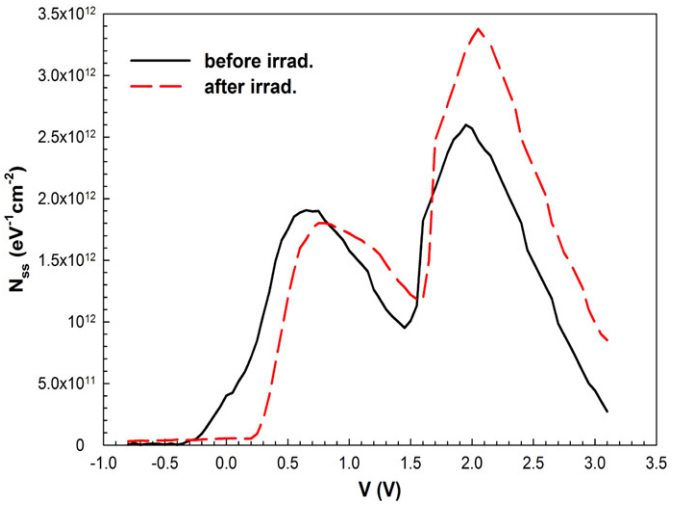

Fig. 6. N_{ss} profile of Au/Polyvinyl Alcohol (Ni, Zn-doped)/n-Si SBD before and after radiation.

C-V and G/ω data of Au/PVA (Ni,Zn-doped)/n-Si SBDs before and after irradiation at room temperature and 1 MHz. The complex permittivity can be expressed as (Daniel, 1967; Symth, 1955):

$$\varepsilon^*=\varepsilon'-j\varepsilon'' \tag{5}$$

where ε' and ε'' are the real and imaginary parts of complex permittivity, respectively, and j is the standard imaginary unit with the property $j^2=-1$. The complex permittivity formalism has been employed to describe the electrical and dielectric properties. The ε^* formalism, in terms of admittance (Y^*) measurements, is expressed with the following relation (Daniel, 1967; Symth, 1955):

$$\varepsilon^*=\frac{Y^*}{j\omega C_o}=\frac{C}{C_o}-j\frac{G}{\omega C_o} \tag{6}$$

where C and G are the measured capacitance and conductance values of the device, respectively, and ω is the angular frequency ($\omega=2\pi f$) of the applied electric field (Mattson et al., 1999). The values of the ε' were calculated using the measured C values for each bias voltage from the following relation (Chelkowski, 1980; Popescu and Bunget, 1984):

$$\varepsilon'=\frac{C}{C_o}=\frac{C\delta}{\varepsilon_o A} \tag{7}$$

where $C_o=\varepsilon_o A/\delta$ is capacitance of an empty capacitor, A is the rectifier contact area of the structure in cm^2, δ is the interfacial polymer layer thickness and ε_o is the permittivity of free space ($\varepsilon_o=8.85\times10^{-14}$ F/cm). The real part of the dielectric permittivity represents the capacitive behavior of the material; hence high-frequency electrical properties of MIS and MOS type devices in accumulation region describe the dielectric properties of the interfacial insulator or polymer layer. Therefore, the values of ε' are extracted from the strong accumulation region. In the strong accumulation region, the maximal capacitance of the MIS type SBD corresponds to the interfacial polymer capacitance ($C_{ox}=\varepsilon' C_0=\varepsilon'\varepsilon_o A/\delta$); once the interfacial polymer layer thickness (δ) is found from this equation as 55 Å, ε' can easily be found using Eq. (7).

The values of the ε'' were calculated from measured G values for each bias voltage from the following relation (Chelkowski, 1980; Faivre et al., 1999; Popescu and Bunget, 1984):

$$\varepsilon''=\frac{G}{\omega C_o}=\frac{Gd}{\varepsilon_o\omega A}=\varepsilon'\tan\delta \tag{8}$$

where dielectric loss tangent is denoted by $tan\delta$ and can be expressed as (Chelkowski, 1980; Daniel, 1976; Faivre et al., 1999; Symth, 1955; Popescu and Bunget, 1984):

$$\tan\delta=\frac{\varepsilon''}{\varepsilon'} \tag{9}$$

AC electrical conductivity (σ_{ac}) of the polymer can be obtained with the following equation (Mattson et al., 1999; Prabakar et al., 2003; Symth, 1955):

$$\sigma_{ac}=\omega C\tan\delta(\delta/A)=\varepsilon''\omega\varepsilon_o \tag{10}$$

The terms complex impedance (Z^*) and complex electric modulus (M^*) formalisms with regard to the analysis of the dielectric or polymer materials have so far been discussed by several authors and most of them have preferred electric modulus in defining the dielectric properties and conduction mechanisms of these materials (Faivre et al., 1999; Pissis and Kyritsis, 1997; Prabakar et al., 2003). One of the advantages of M^* formalism is that it gives more importance to the elements with the smallest capacitance occurring in the dielectric system. In the context of dielectric data, as offered by Faivre et al. (Faivre et al., 1999), the modulus representation is occasionally used in order to emphasize small features at high frequencies. The data regarding Z^* or

the complex dielectric permittivity ($\varepsilon^*=1/M^*$) can be transformed into the M^* formalism using the following relation (Chattopadhyay and Raychaudhuri, 1992; Faivre et al., 1999; Migahed et al., 2004; Pissis and Kyritsis, 1997; Prabakar et al., 2003):

$$M^* = j\omega C_0 Z^* = \frac{1}{\varepsilon^*} = \frac{\varepsilon'}{\varepsilon'^2+\varepsilon''^2} + j\frac{\varepsilon''}{\varepsilon'^2+\varepsilon''^2} = M' + jM'' \quad (11)$$

where ε', M' are the real and ε'', M'' are the imaginary parts of dielectric permittivity and electric modulus, respectively. The ε^* and M^* representation allows us to distinguish the local dielectric relation. Generally, in order to extract as much information as possible, dielectric relation spectroscopy data are used in the electric modulus formalism introduced by Macedo et al. (Macedo et al., 1972). Also, the determination of the electric modulus of these materials and their variation with applied bias voltage provide valuable information that allows study of the relaxation process for a specific electronic application (Macedo et al., 1972).

Before and after irradiation ε'–V, ε''–V and tanδ-V characteristics of Au/PVA (Ni,Zn-doped)/n-Si (SBDs) are given in Fig. 7 (a-c), respectively. As can be seen in Fig. 7 (a), ε' values increase in the inversion and accumulation regions while they decrease in the depletion region under the effect of radiation. Also, before and after irradiation ε'–V plots have a peak at about 1.5 V because of the effect of R_s and the peak shifts to the high forward bias region under the effect of radiation with a decrease in the peak magnitude. This shows that the N_{ss} is the significant parameter in the depletion and weak accumulation regions whereas R_s is the significant parameter in the strong accumulation region. As can be seen in Fig. 7 (a) and (b), there are some similarities between two plots; they both decrease in the depletion region and increase in the accumulation region. However, the values of ε'' in the inversion region are almost constant under radiation effect contrary to the values of ε' in the same region. This behavior can be attributed to the particular distribution of charges and their restructuring and reordering at interface states under radiation effect. Also, the decrease in the magnitude of the peak in the ε' plot shows that interface states at M/S interface are passivated under radiation effect. Fig. 7 (c) shows the variation of tanδ with applied bias voltage. The variation provides that tanδ gives a distinctive peak, as shown in the inset in Fig. 7 (c), at about 0.8 V before and after irradiation due to particular distribution of interface states at M/S interface.

The voltage dependent real (M') and imaginary (M'') electrical modulus plots of Au/PVA (Ni,Zn-doped)/n-Si SBDs before and after irradiation are given in Fig. 8 (a) and (b), respectively. The values of the M' and M'' decrease considerably particularly in the inversion region whereas they become almost constant in the high forward bias region under the effect of radiation. However, unlike the M' plots, M'' plots have a peak in the depletion region

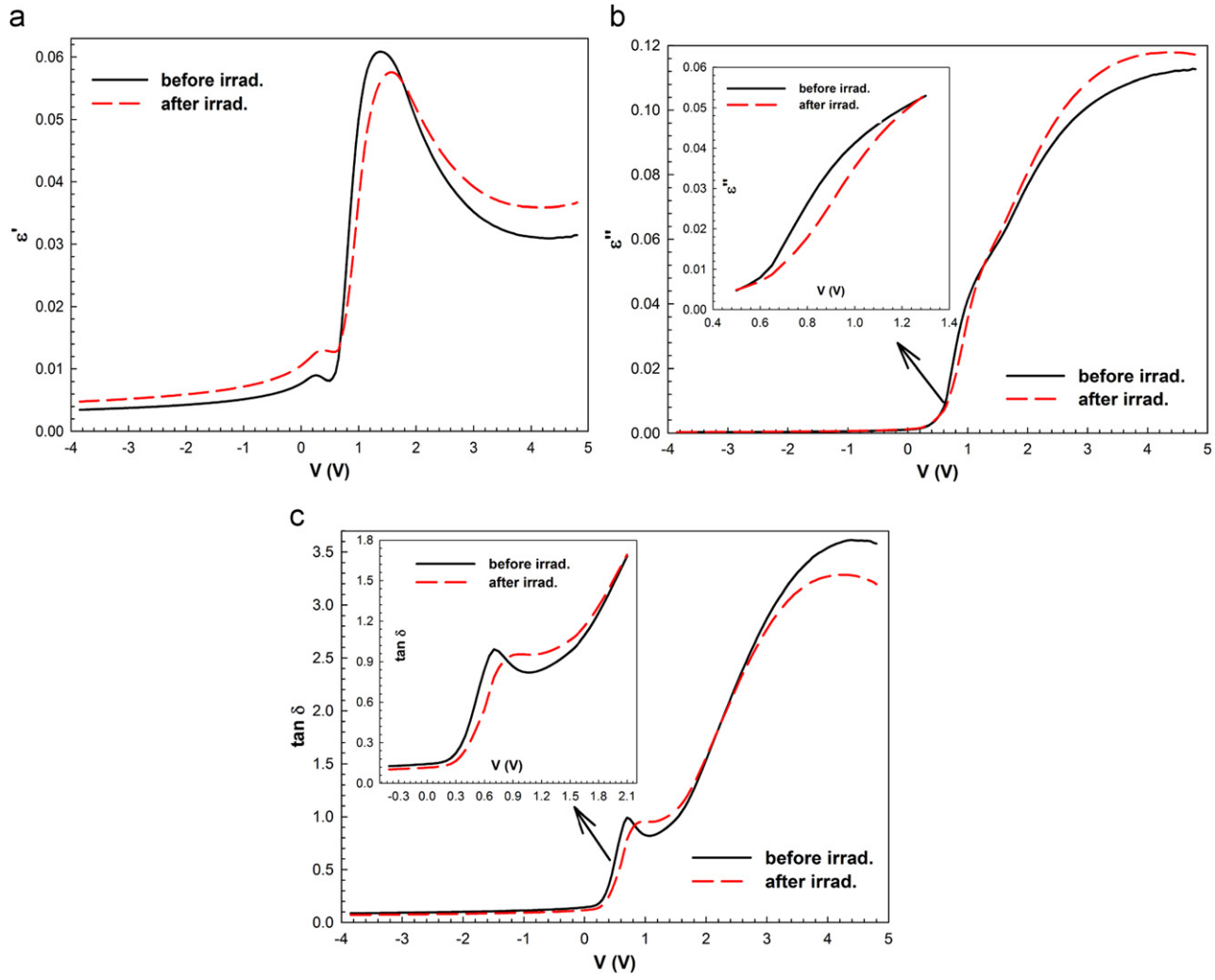

Fig. 7. Voltage dependence of (a) dielectric constant (ε'), (b) dielectric loss (ε'') and (c) loss tangent (tanδ) at room temperature and 1 MHz for Au/Polyvinyl Alcohol (Ni, Zn-doped)/n-Si SBD before and after radiation.

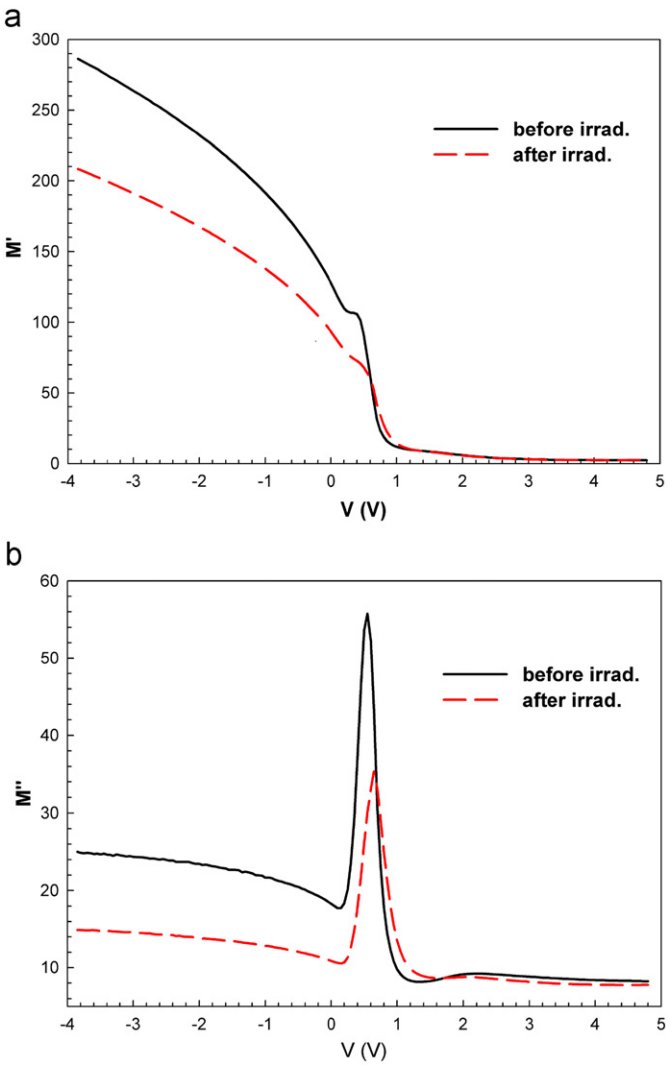

Fig. 8. Voltage dependence of **(a)** the real part M' and **(b)** the imaginary part M'' of electric modulus M^* at room temperature and 1 MHz for Au/Polyvinyl Alcohol (Ni, Zn-doped)/n-Si SBD before and after radiation.

and the magnitude of this peak decreases with radiation effect. It is clear that at 1 MHz the period (T) is very much smaller than the lifetime (τ) of interface states. Therefore, the interface states cannot follow an ac signal and the electrical modulus reaches a maximum value corresponding to $M_\infty = 1/\varepsilon'_\infty$ because of the relaxation process. M'' plots reach a peak value and then decrease to a minimum value. The peak position shifts towards the forward bias region and the magnitude of the peak decreases with γ-ray irradiation since N_{ss} is passivated.

In order to see the effect of γ-ray irradiation on ac conductivity, the σ_{ac}-V plots of the SBD before and after irradiation were obtained from G/ω-V data and are given in Fig. 9. It is seen clearly in Fig. 9 that σ_{ac} is dependent on the radiation and applied bias voltage. As can be seen in the inset in Fig. 9, the values of σ_{ac} decrease in the depletion region while they increase in the strong accumulation region. Such behavior of ac conductivity results from the changes in the conductance under radiation effect and these changes in the strong accumulation region are more distinctive compared to the ones in other regions. Similar results have been reported in the literature [Umana-Membreno et al., 2003; Ma, 1989; Feteha et al., 2002; Winokur et al., 1984; Gökçen et al., 2008] in which the radiation level is kept around the level we used (22 kGy) and even more. As conclusion, despite the fact

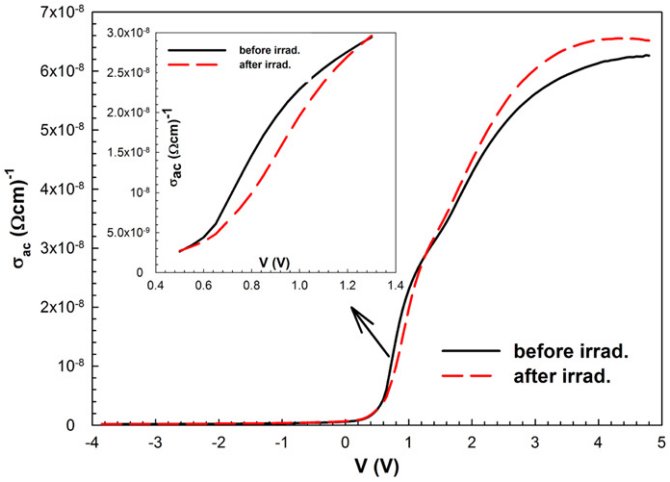

Fig. 9. Variation of the ac electrical conductivity σ_{ac} with applied bias for Au/Polyvinyl Alcohol (Ni, Zn-doped)/n-Si SBD before and after radiation.

that 22 kGy is at intermediate level radiation, this level of radiation caused some changes in the electrical and dielectric properties however these changes are not very serious as this level of radiation does not make the samples unusable, hence it can be said that the fabricated samples in this study are suitable for using in radiation-resistant devices.

4. Conclusion

In order to show the effects of γ-ray irradiation on the electrical and dielectric properties of Au/Polyvinyl alcohol (Ni, Zn-doped)/n-Si SBD, the C-V and G/ω-V measurements were carried out at room temperature and 1 MHz and in the bias voltage range of -4 V to 5 V. Experimental results show that radiation is effective on the C and G values especially in the depletion and accumulation regions. The values of R_s decrease under radiation effect particularly in the inversion region because of the increase in the conductivity of the device. The voltage dependent N_{ss} profile was also obtained from the measured capacitance (C_{HF} and C_{LF}) values method and the values of N_{ss} were found to be about in the order of $10^{12}\,\mathrm{eV}^{-1}\,\mathrm{cm}^{-2}$. In addition, the real and imaginary parts of dielectric constant and electrical modulus, dielectric loss tangent and ac electrical conductivity values were obtained from the measured C and G values before and after irradiation. The changes in the electrical and dielectric properties in the depletion and accumulation regions stem especially from the restructuring and reordering of the charges at interface states, series resistance of device and interfacial polarization. As a conclusion, both electrical and dielectric properties of Au/PVA (Ni, Zn-doped) n-Si SBD are considerably dependent on the radiation and applied bias voltage.

References

Altındal, Ş., Uslu, H., 2011. The origin of anomalous peak and negative capacitance in the forward bias capacitance-voltage characteristics of Au/PVA/n-Si structures. J. Appl. Phys 109 (074503), 1–7.

Akkılıç, K., Uzun, İ., Kılıçoğlu, T., 2007. The calculation of electronic properties of an Ag/chitosan/n-Si Schottky barrier diode. Synth. Metals. 157, 297–302.

Aydın, M.E., Kılıçoğlu, T., Akkılıç, K., Hoşgören, H., 2006. The calculation of electronic parameters of an Au/b-carotene/n-Si Schottky barrier diode. Physica B 381, 113–117.

Aydoğan, Ş., Sağlam, M., Türüt, A., 2005. On the some electrical properties of the non-ideal PPy/p-Si/Al structure. Polymer 46, 10982–10988.

Ahmed, M.A., Abo-Ellil, M.S., 1998. Effect of dopant concentration on the electrical properties of polyvinyl alcohol (PVA). J. Mat. Sci.: Mat. Elec. 9, 391–395.

Card, H.C., Rhoderick, E.H., 1971. Studies of tunnel MOS diodes I. Interface effects in silicon Schottky diodes. J. Phys. D. Appl. Phys. 4, 1589–1601.
Chauhan, R.K., Chakrabarti, P., 2002. Effect of ionizing radiation on MOS capacitor. Microelectron. J. 33, 197–203.
Castange, R., Vapaille, A., 1971. Description of the SiO_2-Si interface properties by means of very low frequency MOS capacitance measurements. Surf. Sci 28 (1), 157–193.
Chelkowski, A., 1980. Dielectric Physics. Elsevier, Amsterdam.
Chattopadhyay, P., Raychaudhuri, B., 1992. Origin of the anomalous peak in the forward capacitance-voltage plot of a Schottky barrier diode. Solid State Electron. 35, 875–878.
Çakar, M., Onganer, Y., Türüt, A., 2002. The nonpolymeric organic compound (pyronine-B)/p-type silicon/Sn contact barrier devices. Synth. Metals 126, 213–218.
Daniel, V.V., 1967. Dielectric Relaxation. Academic Press, London.
Dökme, İ., Altındal, Ş., Tunç, T., Uslu, İ., 2010. Temperature dependent electrical and dielectric properties of Au/polyvinyl alcohol (Ni, Zn-doped)/n-Si Schottky diodes. Microelectron. Reliab. 50, 39–44.
El-Sayed, S.M., Abdel Hamid, H.M., Radwan, R.M., 2004. Effect of electron beam irradiation on the conduction phenomena of unplasticized PVC/PVA copolymer. Rad. Phys. Chem. 69, 339–345.
Faivre, A., Niquet, G., Maglione, M., Fornazero, J., Lai, J.F., David, L., 1999. Dynamics of sorbitol and maltitol over a wide time-temperature range. The Eur. Phys. J. B 10, 277–286.
Feteha, M.Y., Soliman, M., Gomaa, N.G., Ashry, M., 2002. Metal-insulator-semiconductor solar cell under gamma irradiation. Renew. Energy 26, 113–120.
Gomaa, N.G., 2001. Photon-induced degradation in metal-insulator-semiconductor solar cells. Renew. Energy 24, 529–534.
Gökçen, M., Tataroğlu, A., Altındal, Ş., Bülbül, M.M., 2008. The effect of ^{60}Co (γ-ray) irradiation on the electrical characteristics of Au/SnO_2/n-Si (MIS) structures. Rad. Phys. Chem. 77, 74–78.
Gupta, R.K., Singh, R.A., 2004. Schottky diode based on composite organic semiconductors. Mater. Sci. Semicond. Process. 7, 83–87.
Güllü, Ö., Aydoğan, Ş., Türüt, A., 2008a. Fabrication and electrical characteristics of Schottky diode based on organic material. Microelecron. Eng. 85, 1647–1651.
Güllü, Ö., Aydoğan, Ş., Şerifoğlu, K., Türüt, A., 2008b. Electron irradiation effects on the organic-on-inorganic silicon Schottky structure. Nucl. Inst. Meth. Phys. Res. A 593, 544–549.
Hill, W.A., Coleman, C.C., 1980. A single frequency approximation for interface state density determination. Solid-State Electron 23 (9), 987–993.
Jayavel, P., Kumar, J., Santhakumar, K., Magudapathy, P., Nair, K.G.M., 2000. Investigations on the e!ect of alpha particle irradiation-induced defects near Pd/n-GaAs interface. Vacuum 57, 51–59.
Karataş, S., Türüt, A., Altındal, Ş., 2009. Irradiation effects on the C-V and G/ω-V characteristics of Sn/p-Si (MS) structures. Rad. Phys. Chem. 78, 130–134.
Karataş, Ş., Türüt, A., 2010. The frequency-dependent electrical characteristics of interfaces in the Sn/p-Si metal semiconductor structures. Microelectron. Reliab 50, 351–355.
Kubo, J., Rahman, N., Takahashi, Kawai, N.T., Matsuba, Nishida, G.K., Kanaya, Yamamoto, T.M., 2009. Improvement of Poly(vinyl alcohol) Properties by the Addition of Magnesium Nitrate. J. Appl. Poly. Sci. 112, 1647–1652.
Ma, T.P., 1989. Interface trap transformation in radiation or hot-electron damaged MOS structures. Semicond. Sci. Technol. 4, 1061–1079.
Macedo, P.B., Moyniham, C.T., Bose, R., 1972. Role of ionic diffusion in polarization in vitreous ionic conductors. Phys. Chem. Glass 13, 171–179.
Mattson, M.S., Niklasson, G.A., Forsgren, K., Harsta, A., 1999. A frequency response and transient current study of β-Ta_2O_5: Methods of estimating the dielectric constant, direct current conductivity, and ion mobility. J. Appl. Phys. 85 (4), 2185–2191.
Migahed, M.D., Ishra, M., Fahmy, T., Barakat, A., 2004. Electric modulus and AC conductivity studies in conducting PPy composite films at low temperature. J. Phys. Chem. Solids 65, 1121–1125.
Nicollian, E.H., Brews, J.R., 1976. The Si-SiO_2 interface-electrical properties as determined by the metal-insulatör-silicon conductance technique. The Bell Syst. Tech. J. 46 (6), 1055–1138.
Oldham, T.R., McLean, F.B., 2003. Total Ionizing Dose Effects in MOS Oxides and Devices 50 (3), 483–499.
Pissis, P., Kyritsis, A., 1997. Electrical conductivity studies in hydrojels. Solid State Ionics 97, 105–113.
Prabakar, K., Narayandass, S.K., Mangalaraj, D., 2003. Dielectric properties of $Cd_{0.6}Zn_{0.4}Te$ thin films. Phys. Stat. Sol. (a) 199 (3), 507–514.
Popescu, M., Bunget, I., 1984. Physics of Solid Dielectrics. Elsevier, Amsterdam.
Radwan, R.M., 2007. High gamma dose response of the electrical properties of polyethylene terephthalate thin films. Nucl. Inst. Meth. Phys. Res. B 262, 249–254.
Shehap, A., Abd Allah, R.A., Basha, A.F., Abd El-Kader, F.H., 1998. Electrical properties of gamma-irradiated, pure, and nickel chloride-doped polyvinyl alcohol films. J. Appl. Polymer Sci. 68, 687–698.
Symth, C.P., 1955. Dielectric Behavior and Structure. McGraw-Hill, New York.
Taşcıoğlu, İ., Tataroğlu, A., Özbay, A., Altındal, Ş., 2009. The role of ^{60}Co γ-ray irradiation on the interface states and series resistance in MIS structures. Rad. Phys. Chem. 79, 457–461.
Taşcıoğlu, İ., Uslu, H., Altındal, Ş., Durmuş, P., Dökme, İ., Tunç, T., 2010. The Effect of Gamma Irradiation on Electrical Characteristics of Au/Polyvinyl Alcohol (Co, Zn-Doped)/n-Si Schottky Barrier Diodes. J. Appl. Polym. Sci. 118, 596–603.
Tunç, T., Altındal, Ş., Dökme, İ., Uslu, H., 2011. Anomalous Peak in the Forward-Bias C-V Plot and Temperature-Dependent Behavior of Au/PVA (Ni, Zn-doped)/n - Si(111) Structures. J. Electron. Mater. 40, 157–164.
Uslu, H., Altındal, Ş., Tunç, T., Uslu, İ., Mammadov, T.S., 2011. The illumination intensity and applied bias voltage on dielectric properties of Au/Polyvinyl Alcohol (Co, Zn-doped)/n-Si Schottky barrier diodes. J. Appl. Polym. Sci. 120, 322–328.
Uslu, H., Altındal, Ş., Dökme, İ., 2010. Illumination effect on electrical characteristics of organic-based Schottky barrier diodes. J. Appl. Phys. 108 (104501), 1–6.
Uğurel, E., Aydoğan, Ş., Şerifoğlu, K., Türüt, A., 2008. Effect of 6 MeV electron irradiation on electrical characteristics of the Au/n-Si/Al Schottky diode Microelecron. Eng. 85, 2299–2303.
Umana-Membreno, G.A., Dell, J.M., Parish, G., Nener, B.D., Faraone, L., Mishra, U.K., 2003. ^{60}Co Gamma Irradiation Effects on n-GaN Schottky Diodes. IEEE Trans. Electron. Dev. 50 (12), 2326–2334.
Vural, Ö., Yıldırım, N., Altındal, Ş., Türüt, A., 2007. Current-voltage characteristics of Al/Rhodamine-101/n-GaAs and Cu/Rhodamine-101/n-GaAs rectifier contacts. Synth Metals 157, 679–683.
Winokur, P.S., Schwank, J.R., McWhorter, P.J., Dressendorfer, P.V., Turpin, D.C., 1984. Correlating the radiation response of MOS capacitors and transistors. IEEE Trans. Nucl. Sci. NS-31 (6), 1453–1460.
Winokur, P.S., McGarrity, J.M., Boesch, H.E., 1976. Dependence of interface-state buildup on hole generation and transport in irradiated MOS capacitor. IEEE Trans. Nucl. Sci. NS-23, 1580–1585.
Yufen, W., Xisolong, C., Yaonan, L., 1994. Radiation effects on dielectric properties of polymer films. IEEE Int. Symp. Elect. Insul., 368–371.
Yamaguchi, M., 2001. Radiation-resistant solar cells for space use. Sol. Energ. Mat. Sol. C. 68, 31–53.
Zainninger, K.H., Holmes-Siedle, A.G., 1967. A Survey of Radiation Effect in MIS Devices, RCA Rev.